

# Virtual DMT: An Opportunity for Pile Design?

Gianni Togliani

<sup>1</sup> *Geologist, Gradinata Forghèe 2- 6900 Massagno (CH), gtoliani @bluewin.ch*

**Abstract – The DMT results are rarely used for piles design, probably because its diffusion and popularity are still limited although DMT is in use for a long time. Conversely CPTu are much more popular and often used to this purpose: this is the reason why a large concerned database is available where it is possible to get the CPTu/DMT conversion experienced in recent years. This was done for two well-documented cases [a bored pile in Santa Cruz (Bolivia) and a driven pipe pile in Sandpoint, (US)] with promising results.**

## I. INTRODUCTION

The DMT is much less popular than CPTu despite its use since 1978 and it is one of the few, among the commercial in situ test, whose measurements are remarkably affected by stress history.

This lesser notoriety overall penalizes the deep foundations design, being very rare the papers that use DMT data to this purpose; on the contrary the database available for CPTu is enviably vast.

The availability of correlations that allow the CPTu/DMT conversion [1], [2], [3], [4] and [5], also allow us to take advantage of the cited database and to make Class C predictions about pile capacity and its load-displacement curves using virtual DMT.

This exercise is considered helpful in prospective because it not only suggests a method applied to an in situ test of great potentials but it also promotes its use being obvious that the best results will be obtained by a real DMT.

In fact, on this subject, we emphasize that being the unit friction activated in a pile at relatively small strains,  $p_0$ , the lift-off pressure, is certainly appropriate because precisely determined in this domain, while  $p_1$ , the expansion pressure, measured at large strains, is undoubtedly more appropriate than the cone penetration resistance  $q_c$ , a failure value, to estimate its toe unit resistance.

Thanks to the courtesy of Dr. Bengt Fellenius who has made available the CPTu data used in two of his papers/presentations on this subject [6], [7], it has been possible to derive the corresponding virtual DMT which have allowed the prediction of the pile capacity and of the load-displacement curves both of a driven pile ( $D=0.406m$ ,  $L=45m$ ) installed at Sandpoint (Idaho-US)

and a bored pile ( $D=0.6m$ ,  $L=16.4m$ ) carried out in an experimental test site in Santa Cruz (Bolivia).

Afterward, these predictions are compared with measurements and with results obtained by other methods which directly employ the CPTu outcomes.

The documents mentioned above (No. 255/259 and No. 348) are available on [www.fellenius.net/](http://www.fellenius.net/).

## II. PILE DESIGN METHODS BASED ON CPTU/DMT

With regard to methods based on CPT/CPTu, Niazi & Mayne [8] in their document on the state of the art (2013), discuss their evolution in the last 60 years focusing on about thirty of them detailing their main characteristics and basic equations.

Among these, the ones proposed by LCPC, Eslami & Fellenius, KTRI and Togliani were chosen to compare their results but only the latter has been updated as follows.

The Author method is based on  $q_c$  and on the friction ratio  $R_f$  and therefore also on the skin friction  $f_s$  a parameter which has a lower reliability than  $q_c$ .

As a consequence, for control purposes, a new method predominantly based on  $q_c$  but using also  $\Delta u$  (the difference between the piezocone and the hydrostatic pore pressure) and  $f_s$ , as subdivision criteria for soils with different behaviour, is proposed.

In this regard it was assumed that " $\Delta u < 100$  kPa" is the proper limit to separate the cohesionless and the cohesive overconsolidated soils from normally (NC) or slightly overconsolidated (LOC) soils and that  $f_s < 20$  kPa particularly indicates the soft/very loose geomaterials.

Of course the other parameters that have been used as shear waves velocity ( $v_s$ ), unit weight ( $\gamma_T$ ), shear modulus at small strain ( $G_0$ ), and overconsolidation ratio (OCR), were obtained using correlations based solely on  $q_c$ .

For the Author's method the resistance equations are the following:

$$\text{Shaft } R_{\text{shaft}} = \sum [(d_{\text{aver}} \cdot h_i \cdot q_s)] \quad (1)$$

$$\text{Taper } R_{\text{taper}} = \sum [(1/4)(d_{\text{top}}^2 - d_{\text{bottom}}^2) q_c K (d_{\text{aver}}/d_{\text{base}})] \quad (2)$$

$$\text{Toe } R_{\text{toe}} = [(1/4)d_{\text{base}}^2 \cdot q_b] \quad (3)$$

where:  $h_i$  = layer thickness;  $d_{\text{aver}} = (d_{\text{top}} + d_{\text{bottom}})/2$ ;  $d_{\text{base}}$  = toe diameter

The reference equation for the toe unit resistance ( $q_b$ )

evaluation is the same for both methods:

$$q_b = q_{c,base} [\lambda + (0.005 L_{pile}/d_{base})] \quad (4)$$

with  $q_{c,base}$  measured from  $+8d_{base}$  to  $-4d_{base}$

while those for the unit friction resistance ( $q_s$ ) are respectively:

#### A. CPTu Original Method ( $q_c, R_f$ )

$$\text{If } f_s < 20 \text{ kPa} \quad q_s = \beta q_c^{0.4} \quad (5)$$

$$\text{If } R_f > 1.5 \quad q_s = \beta \{q_c^{0.52} [1.1(0.4 + \text{LN}(R_f))]\} \quad (6)$$

$$\text{If } 1 < R_f < 1.5 \quad q_s = \beta \{q_c^{0.51} [0.8 + (1 - R_f)/8]\} \quad (7)$$

$$\text{otherwise} \quad q_s = \beta \{q_c^{0.53} [0.8 + (1.1 - R_f)/8]\} \quad (8)$$

#### B. CPTu Control Method ( $q_c$ )

$$\text{If } \Delta u < 100 \text{ kPa} \quad q_s = \beta q_c^{0.48 + \alpha} \quad (9)$$

$$\text{where } \alpha = 0.06 \text{LOG}(\text{OCR}) \quad (10)$$

$$\text{If } f_s < 20 \text{ kPa} \quad q_s = \beta q_c^{0.40} \quad (11)$$

$$\text{otherwise} \quad q_s = \beta q_c^{0.50} \quad (12)$$

$$\text{and} \quad q_{s,final} = \beta (q_s \sigma'_v)^\delta \quad (13)$$

$$\text{where } \delta = 0.020 \text{ (} L_{pile} < 10\text{m)}$$

$$\delta = 0.025 \text{ (} L_{pile} < 20\text{m)}$$

$$\delta = 0.030 \text{ (} L_{pile} < 30\text{m)}$$

$$\delta = 0.035 \text{ (} L_{pile} < 40\text{m)}$$

$$\delta = 0.040 \text{ (} L_{pile} < 50\text{m)}$$

The DMT pile capacity prediction method refers instead to paper [9] whose equations have been partially updated as specified below:

$$\text{If } I_D > 1.8 \quad q_s = \beta (p_0^{0.68} K_D^{0.3} I_D^{0.4}) \quad (14)$$

$$\text{If } 0.6 < I_D < 1.8 \quad q_s = \beta (p_0^{0.66} K_D^{0.3}) \quad (15)$$

$$\text{If } I_D < 0.6 \quad q_s = \beta (p_0^{0.55} K_D^{0.1} I_D^{0.4}) \quad (16)$$

where  $I_D$  is the material index and  $K_D$  is the horizontal stress index

$$\text{If } p_1 \quad q_b = p_{1,base} [\lambda + (0.005 L_{pile}/d_{base})] \quad (17)$$

$$\text{otherwise} \quad q_b = p_{1,base} \quad (18)$$

with  $p_{1,base}$  measured from  $+8d_{base}$  to  $-4d_{base}$

Finally, for the coefficients  $\beta, \lambda, \epsilon, \kappa$ , the selected values depending on piles type are summarized in the following table.

Table 1. Piles Type Factors

Pile Type	$\beta$	$\lambda$	$\kappa$
Precast Driven/Jacked	1.00	0.30	1.3 to 1.1
			Function of $q_c$
D.D. (e.g. Bauer, Omega)	0.90	0.25	
Pipe (Open End)	0.70	0.20	
HP	0.65	0.15	
CFA, Bored (polymer)	0.60	0.10	
Bored (bentonite, cased)	0.50	0.10	

### III. BORED PILE ( $D=0.6\text{M}$ , $L.=16.4\text{M}$ )

This pile (TP1) has been drilled on April 20th, 2015, by pushing a temporary casing into the ground while augering out the core as the pipe is advanced.

Once the pipe reached its design depth and had been augered out, concrete was poured into the pipe while it was extracted and then a reinforcing cage with 0.45m outside diameter was inserted into the pipe.

The cage was instrumented with three levels of a strain-gage at depth 1.80 m, 9.30 m, and 13.80 m below ground surface.

A 310 mm high pressure hydraulic jack was attached to the cage to serve as a bidirectional cell (BDC) in the first phase of the loading test.

Thus, in the test, the pile would be separated in an upper 14.8 m length and a lower 1.6 m long section: telltale guide pipes were attached to the cage so as to measure the opening of the BDC and movement of the lower end of the same.

The static loading test was performed in two phases: Phase 1, the bidirectional test, on May 7, 2015 while Phase 2 consisted in leaving the BDC open (free-draining), was carried out on May 8, 2015 realizing a head-down test by means of a conventional reaction pile arrangement.

TP2, a twin pile (equal length and size), was constructed on the same day 5 m away from TP1: it was tested as a full-length pile after the TP1.

More details can be found in the document No. 348 cited on page 1.

The derived  $I_D$  and  $K_D$  values are shown in Figure 1 together with the correlations used while the plot of Figure 2 combines the measured CPTu parameters and  $p_0$  e  $p_1$  instead obtained from  $I_D$  and  $K_D$  (virtual DMT) to verify their consistency (e.g.  $p_0$   $u_2$  in cohesive NC/LOC soils).

The subsoil lithological characterization or better its mechanical behaviour (SBT) is represented in Figure 3 while Figure 4 shows the values trend for unit weight ( $\gamma_T$ ), shear waves velocity ( $V_s$ ), shear modulus ( $G_0$  or  $G_{max}$ ) and elastic modulus ( $E_0$  or  $E_{max}$ ) at small strain, all necessary both for the CPTu/DMT conversion and for piles capacity and load-displacement curve predictions.

The outcome of the different methods used are compared in Figure 5: it can be noticed that those of the Author have final values very similar to each other despite the trend of DMT method deviates from those using CPTu; the others provides a lower shaft resistance but matching their capacity (LCPC) or exceeding the same (Eslami & Fellenius) by virtue of a higher toe resistance.

The load-displacement curve simulation based on processing the virtual DMT pile capacity results, was made using the elastic continuum theory, as presented by [10], [11] and [12]) and described in [13]; the modulus

decay with the strain increase was modelled using the Fahey & Carter (1993) [14] equation (modified hyperbola).

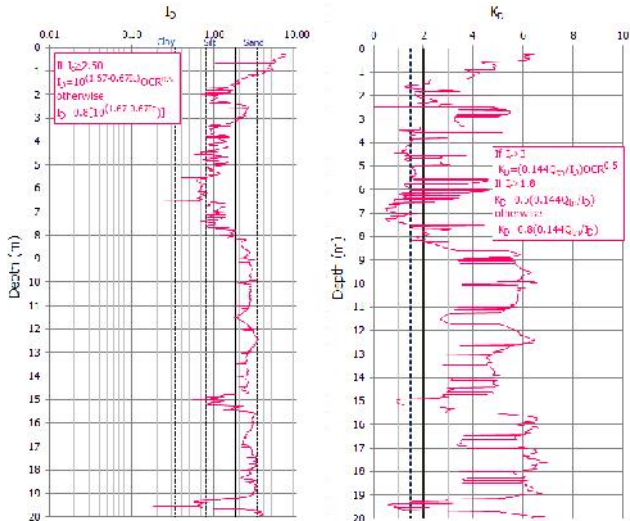


Fig. 1.  $I_D$  &  $K_D$  Plots

It is also to remember that the operational values chosen for the soils elastic moduli at mid-length ( $E_{SM}$ ), and at pile base ( $E_{SL}$ ), are not exactly those obtainable from the specific graph of Figure 4: they are higher for driven piles (the soil immediately surrounding is densified) and lower for bored piles following to the decompression due to soil removal.

It is also emphasized that the pile reference capacity was chosen not as by Eurocodes specified at pile head movement equal to 10% of its diameter, but rather a value corresponding to 30 mm of pile head displacement was assumed (for Dr. Fellenius such movement should be chosen on toe curve).

The pile service capacity was then derived reducing the obtained load by means of a safety factor depending on the displacement and on the pile diameter basing on the equation shown in Figure 6 (left graph).

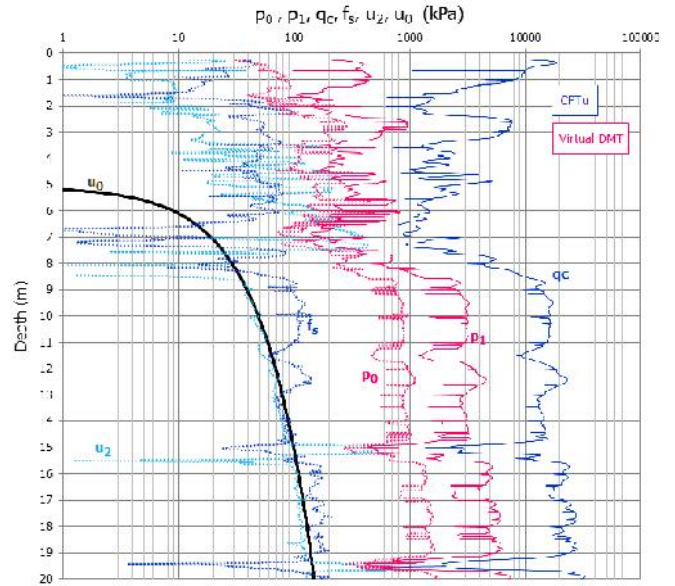


Fig. 2. Synoptic Plots

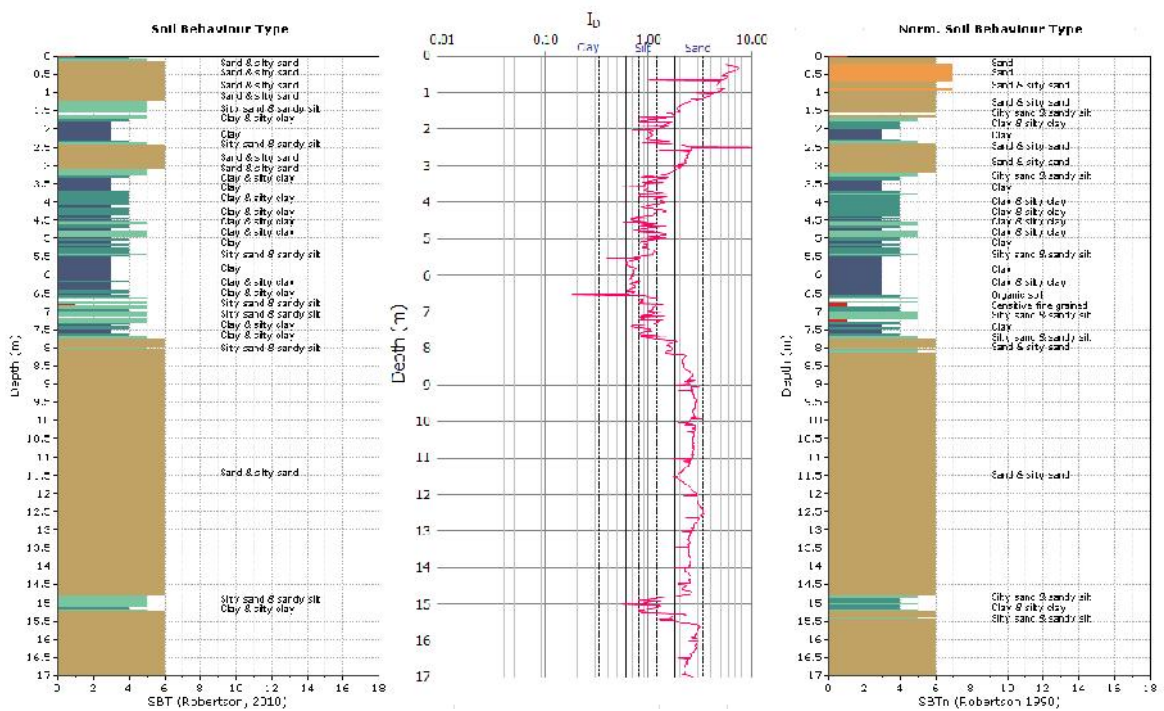


Fig. 3. SBT Lithology

The intersection with the toe capacity line allows the plotting of the load distribution curve with depth at a toe movement of 3.8mm and 25.5mm respectively as shown in Figure 6 (right graph).

It is interesting to note that the mobilized shaft and toe resistances are equal to 62% and 33% of the total for a toe displacement of 3.8mm and to 90% and 87% at a toe displacement of 25.5mm.

Finally, considering that the load-displacements curves of TP1 and TP2 show not negligible differences, despite of the fact that they are “twins”, it is believed that the approximation of the simulated curve is good, at least up to the movement considered as allowable, after all as requested by a Class C prediction and are therefore also good the capacities (shaft and toe) obtained from the virtual DMT employed to this purpose.

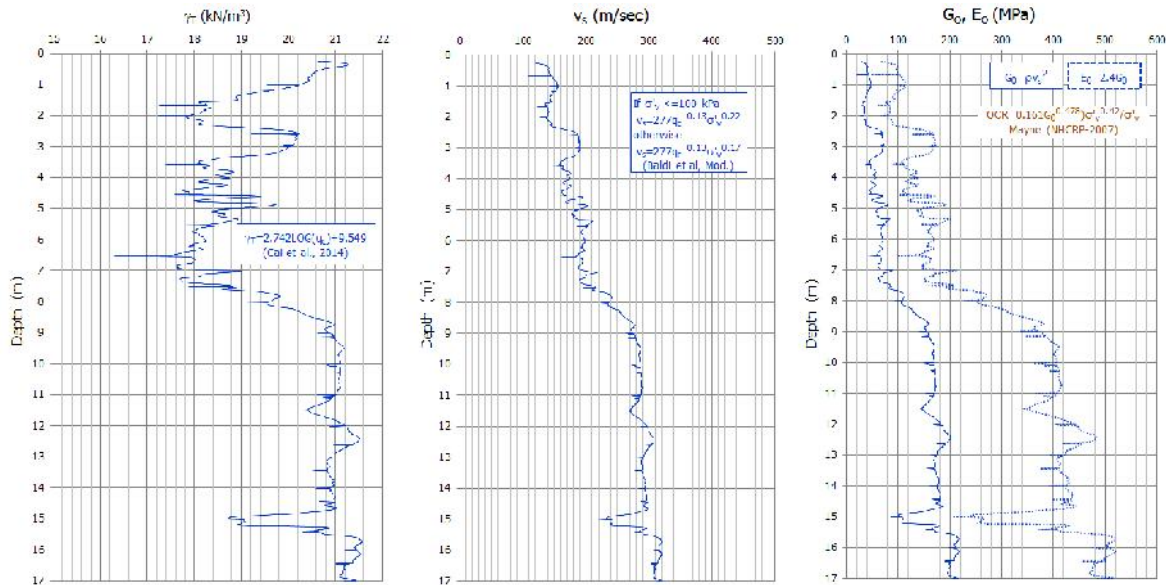


Fig. 4, Unit Weight, Shear Waves Velocity, Moduli

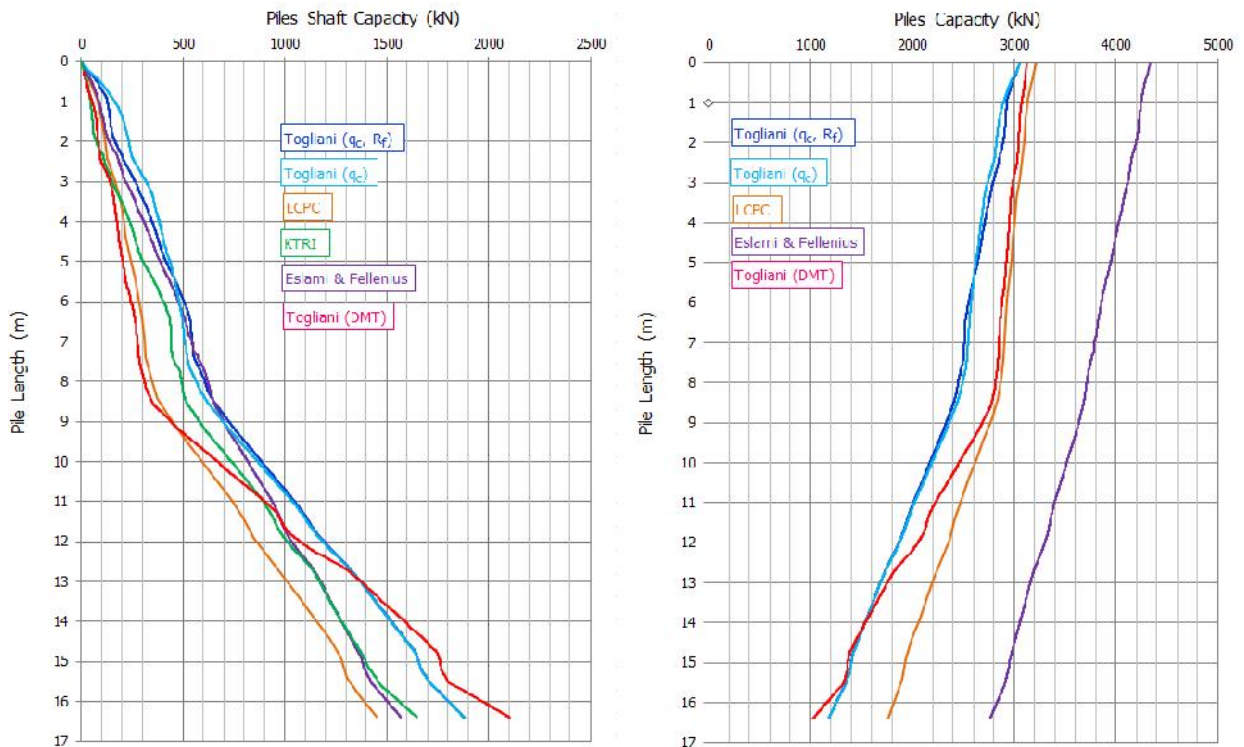


Fig. 5, Piles Capacities Comparisons

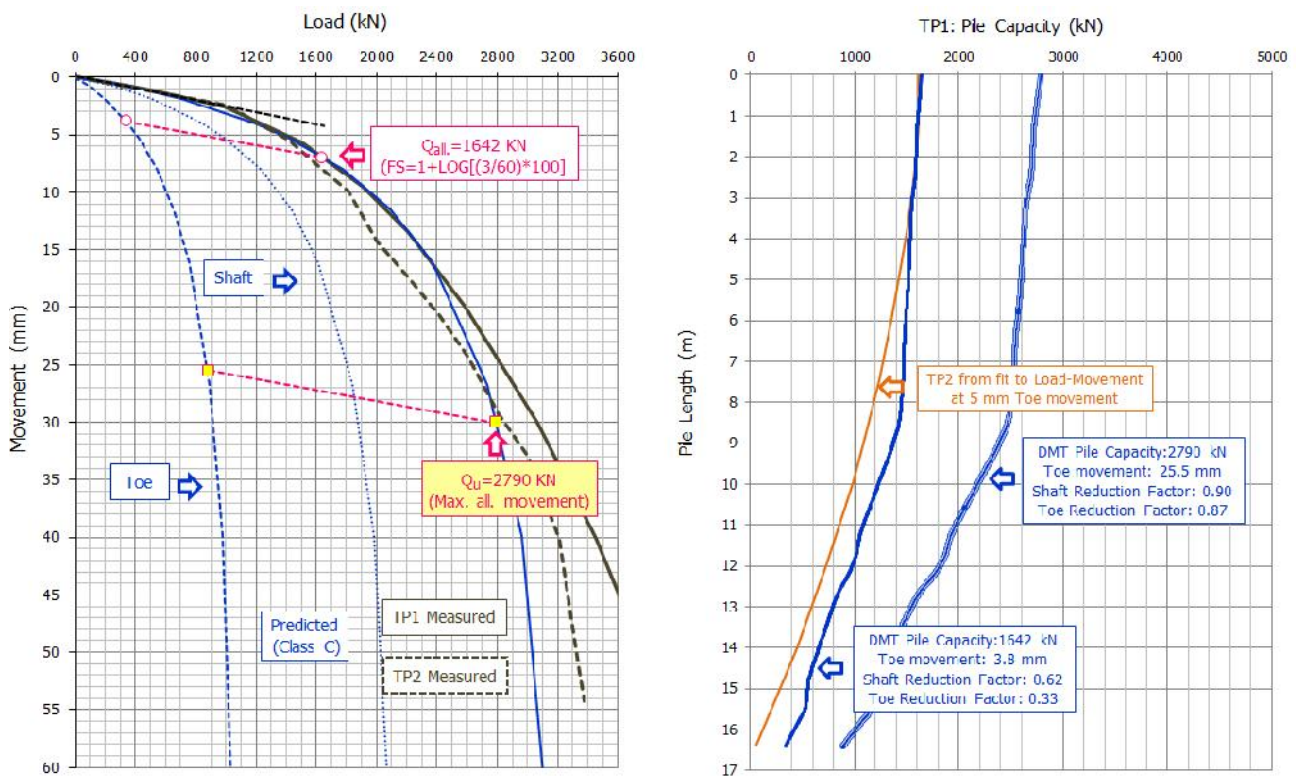


Fig. 6. Load –Movements and Load Distribution Curves

#### IV. DRIVEN PIPE PILE (D=0.406M, L.=45M)

The soils at the site are post-glacial alluvial deposits with a thickness estimated to exceed 65 m consisting in sequence of silty sand/sandy silt (9 m), soft silty clays locally with silty sandy layers (40 m) and by alternating silt, sandy silt, silty clay (17 m); the water table lies 4/4.50 m below ground level.

A closed-toe steel pipe, 12.5 mm thick, was driven on August 31, 2001 with an APE D36-32 single-acting diesel hammer to an embedment depth of 45.0 m.

The pile was instrumented at eight levels with vibrating wire strain gages (at 0.4 m, 5.6 m, 9.2 m, 16.0 m, 23.0 m, 30.0 m, 37.1 m and 44.0 m below ground level); before of the pile concreting two 25 mm outer diameter (OD) pipes were installed inside the pile as guides for telltales: the tip of the deeper one was placed at the pile toe while the other 6.45 m above with the purpose of obtaining the shortening of the pile between head and toe.

Dynamic monitoring with the Pile Driving Analyzer (PDA) was carried out both during installation and once the full embedment was reached: the end-of-driving and the 16-hour restrike CAPWAP capacities were 260 kN and 980 kN, respectively.

The static loading test was carried out 46 days after the

driving to be sure that the pore pressure induced by pile driving had been totally dissipated; its values were measured via vibrating wire piezometers installed approximately 1.2 m away from the surface of the pile.

As for the previous case, first the CPTu derived  $I_D$  and  $K_D$  values are represented in Figure 7, again with the correlations used, while in Figure 8 the graph plots together the CPTu measured parameters and  $p_0$  and  $p_1$  obtained via  $I_D$  and  $K_D$ , for the usual consistency verifications; from their analysis it is immediately evident that the sleeve friction values ( $f_s$ ) of the intermediate silty clays are abnormally low.

It is worth to note that the above sleeve friction values may lead to erroneous conclusions if used, for example as often occurs, for the evaluation of the unit weight: being these significantly lower than laboratory data (Fig.9), one could end up with a lithostatic pressure unrealistically low and a consequent overestimation of the related OCR.

It is also quite unusual that the pore pressure measured values ( $u_2$ ), match or are very near to the point resistance ( $q_c$ ).

All of this offer some explanation to the fact that from 10 to 40 m depth  $p_0$  and  $p_1$  values are between  $u_0$  and  $u_2$  and not close to or above the latter, as they should.

The lithology classification derived from SBT confirms the stratigraphic sequence of the three formations

previously described.

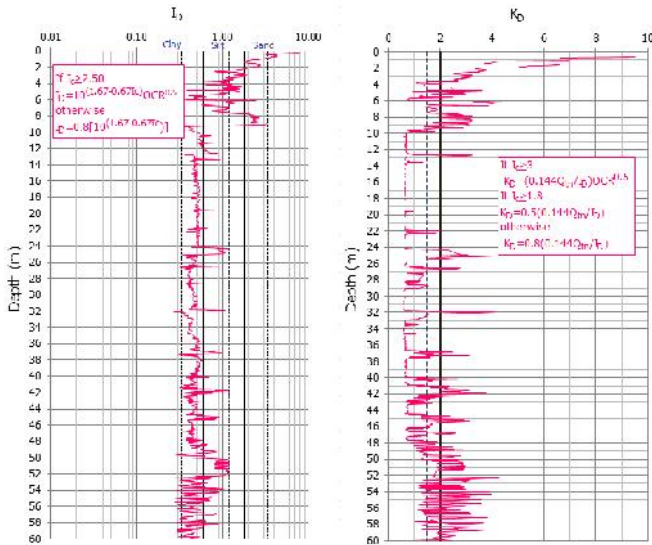


Fig. 7.  $I_D$  &  $K_D$  Plots

Figure 9 shows the parameters (unit weight, shear waves velocity and moduli at low strain) necessary for all of the numerical analyses carried out.

The different prediction methods outcome are compared in Figure 10 where the analysis shows that the final resistance values are very much alike and near to the measured ones although the followed paths are not similar.

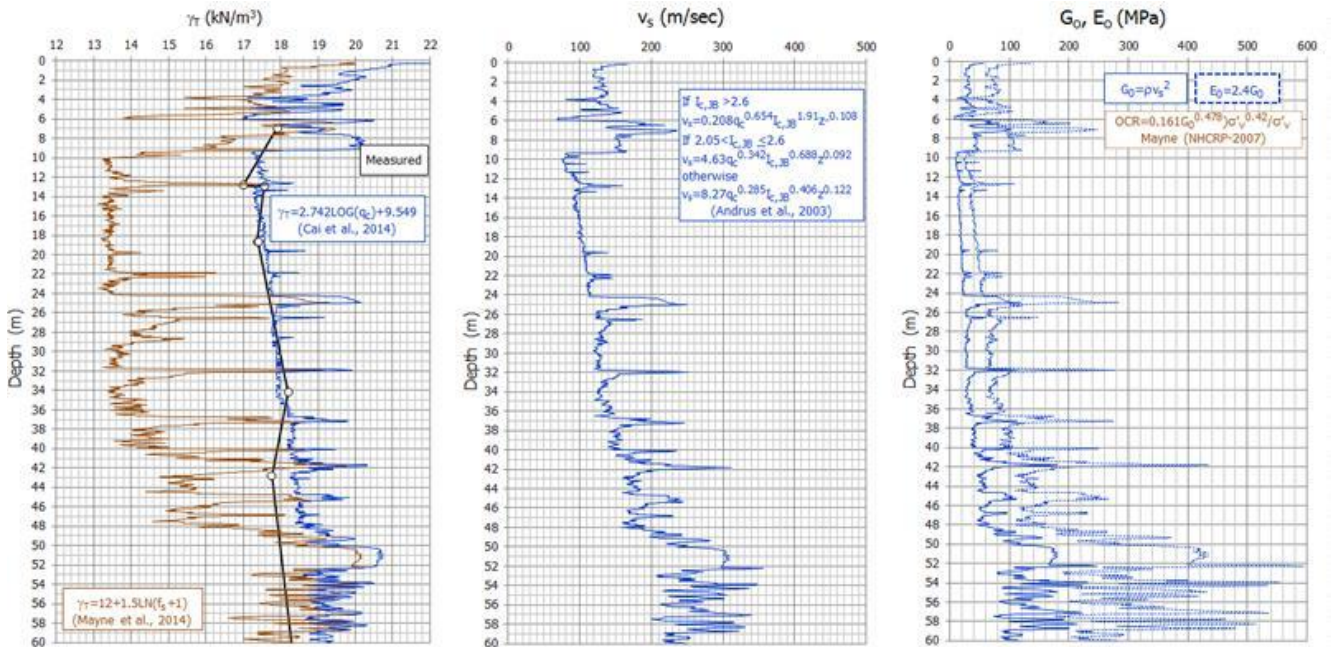


Fig. 9. Unit Weight, Shear Wave Velocity, Moduli

The exception is KTRI method, directly exploiting the sleeve friction values, which is significantly underestimating the resistance, as indeed might be expected.

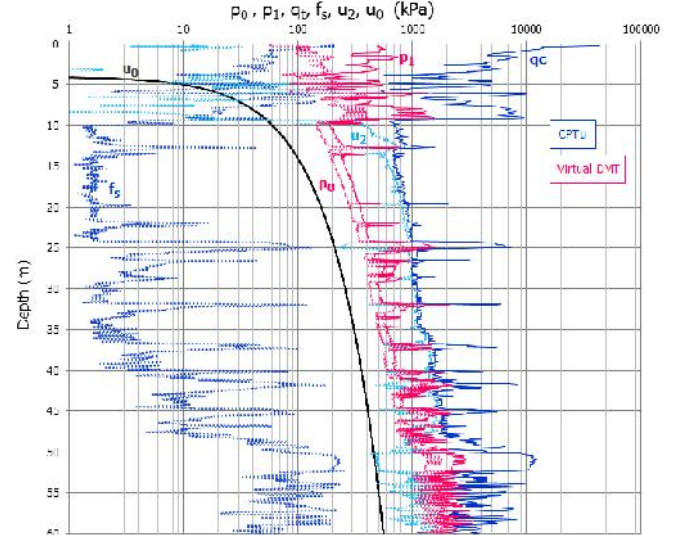


Fig. 8. Synoptic Plots

However, the distribution of measured resistance leads to some doubts lacking a reasonable justification (residual stresses?) of their almost vertical trend between 31 m and 45 m depth.

As in the previous case the pile capacity has been chosen on the simulated load-displacement curve at 30 mm settlement and the allowable capacity is obtained by the same procedure described for Santa Cruz pile (Figure 11).

This time, the parallel to the elastic compression line intersects the toe resistance curve at a displacement equal to 1.8mm and 27.7 mm respectively, mobilizing toe and shaft resistances in the first case equal to 12% and 57% of total and in the second to 96% and 99%

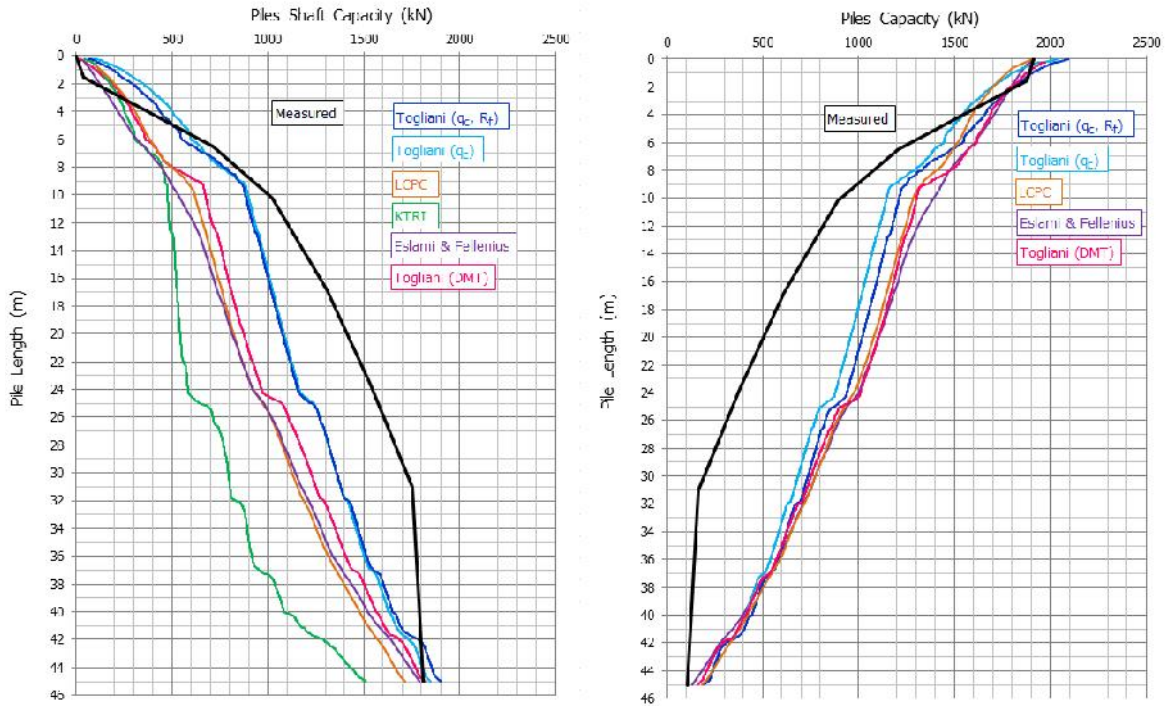


Fig.10. Piles Capacities Comparisons

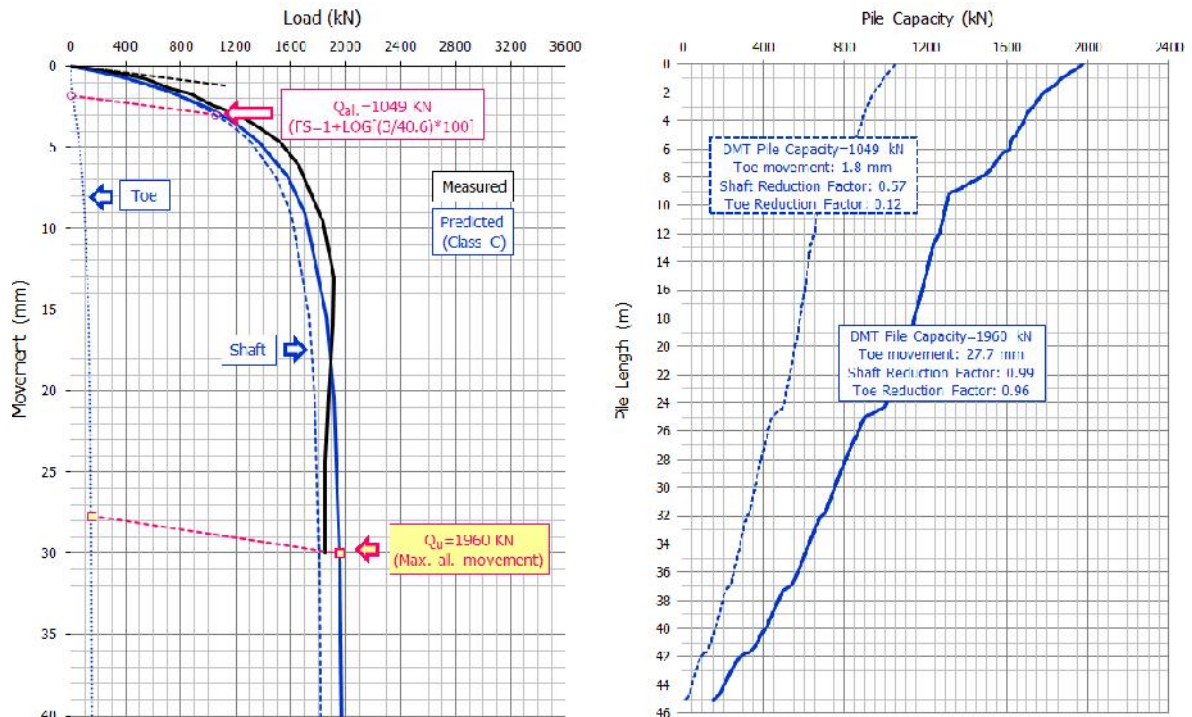


Fig. 11. Load-Movement and Load Distribution Curves

Finally, with reference to what so far discussed, it seems reasonable to state that even in this case the method based on virtual DMT provides reliable results both for the resistance mobilized by the test pile and for the simulated load-displacement curve.

## V. CONCLUSIONS

The described cases are very different not only for type and size of the test piles but also and specifically for the lithological/geomechanical soils characteristics: however it has been shown that the virtual DMT can effectively be employed for their design and, as a logical consequence, that it will be possible to obtain even better results with a real DMT.

Therefore, the use of virtual DMT has not been proposed to recommend it as common practice but only as a stimulation to the combined use of CPTu and DMT in site investigation.

In addition to a better subsoil geotechnical characterization, two in situ exploration tools of extreme importance for deep foundations design, would in fact always be available, able to create a mutual synergy arguably effective to reduce to acceptable terms the excessive results dispersion presently encountered in piles capacity estimate also because of the lack of shared guidelines about head displacements and time of reference.

## VI. ACKNOWLEDGMENTS

Many thanks are addressed to Dr. B.H. Fellenius for having made available the data necessary for the paper editing, as well as to Dr. L. Albert and to Prof. P. Monaco for their critical review.

## REFERENCES

- [1] Mayne, P.W. 2002. Equivalent CPT method for calculating shallow foundation settlement in the Piedmont residual soils based on the DMT constrained modulus approach. *geosystems*. ce.gatech.edu/Faculty/Mayne/
- [2] Mayne, P.W. 2006. Interrelationship of DMT and CPT readings in soft clays. *Proceedings DMT'06*. Washington, D.C., April 2-5, 2006.
- [3] Robertson, P.K. 2009 "CPT-DMT Correlations," *Journal of Geotechnical and Geoenvironmental Engineering*, ASCE, Vol. 135, No. 11, November, 2009, pp. 1762-1771
- [4] Robertson, P.K. 2015. Soil Behaviour Type using the DMT. *Proceedings DMT'15*. Rome, June 14-16, 2015.
- [5] Togliani, G., Calzolari L. and Menghini A. 2015 Governolo (Italy) Experimental Site: In Situ Tests Comparisons and Mutual Conversions. *Proceedings DMT'15*. Rome, June 14-16, 2015.
- [6] Fellenius B.H., 2015. Field Tests and Prediction. *Secundo Congreso Internacional de Fundaciones Profundas de Bolivia*. Santa Cruz May 12-15. Lecture 22 p.
- [7] Fellenius B.H., Harris D. and Anderson D.G. 2003. Static loading test on a 45 m long pipe pile in Sandpoint, Idaho. *Canadian Geotechnical Journal* 41(4), 613-628
- [8] Niazi, F.S. and Mayne, P. W. 2013. *Cone Penetration Test Based Direct Methods for Evaluating Static Axial Capacity of Single Piles*. Springer
- [9] Togliani, G. and Reuter, G.R. 2015 *Piles Capacity Predictions (Class C): DMT vs CPTu*. *Proceedings DMT'15*. Rome, June 14-16, 2015.
- [10] Randolph, M.F. and Wroth C.P. 1978. Analysis of deformation of vertically loaded piles. *Journal of the Geotechnical Engineering Division ASCE*. Vol.104 (GT12),1465-1488
- [11] Randolph, M.F. and Wroth, C.P. 1979. A simple approach to pile design and the evaluation of pile tests. *Behavior of Deep Foundation*, STP 670, ASTM, 484-499
- [12] Poulos, H.G. (1979) "Foundation Settlement Analysis Using Elastic Theory". In *The Profession of a Civil Engineer*, Ed. D. Campbell-Allen and E.H. Davis, pp. 119-146, Sydney University Press.
- [13] Mayne, P. W. and Schneider, J.A. 2001. Evaluating Axial Drilled Shaft Response by Seismic Cone. *Foundation and Ground Improvement, GSP 113*, ASCE, Reston/VA: 655-669.
- [14] Fahey, M. and Carter, J. 1993. A finite element study of the pressuremeter using a nonlinear elastic plastic model. *Canadian Geotechnical Journal* 30(2), 348-362